PKD1 participates in the processing of aortic dissection via regulating vascular smooth muscle cell contraction and MAPK signaling

Junbo Feng[*], Yuntao Hu, Peng Peng, Juntao Li, Shenglin Ge

Department of Cardiovascular Surgery, The first affiliated hospital of Anhui Medical University, Hefei, China

ARTICLE INFO

ABSTRACT

Aortic Dissection (AD) is a cardiovascular emergency with high mortality, of which one feature is the phenotypic switch of vascular smooth muscle cells (VSMCs). Transient Receptor Potential Channel Interacting (*PKD1*) has been regarded as one regulator as well as one biomarker for AD. However, multiple candidate pathways were reported through which *PKD1* regulates AD in previous studies, but a comprehensive insight is still absent. In this study, we compared the AD and normal samples in transcriptome scale and detected 717 *PKD1*-related differential expressed genes, which enriched in mitogen-activated protein kinase (MAPK) signal transduction (AD tissue preference) and VSMC contraction pathway (normal tissue preference). Furthermore, we also found two important functional hub genes in *PKD1* regulation, *JUN* and *ACTN2*, and established a carnal-miRNA-mRNA network. Our study demonstrated the co-regulation of muscle development and signal transduction in AD's progression and also provided the genetic basis for the following mechanism research with AD.

Introduction

Aortic Dissection (AD) is characterized as a tear within the intimal layer of the aorta, causing separation of the intimal and medial layers of the aortic wall (1). As the major cell type in aortic tissue, vascular smooth muscle cells have two phenotypes, contractile and synthetic. The phenotypic switch from contractile to synthetic vascular smooth muscle cells (VSMCs), with the increase of proteolytic enzyme production, is a key alteration in AD development. The infiltration of inflammatory cells and endoplasmic reticulum stress induced by mechanical wall stress are associated with VSMCs apoptosis, which may also contribute to AD development and progression (2,3). The previous study also evidenced that the mitogen-activated protein kinase (MAPK) signaling pathway, which may regulate cellular apoptosis and stress responses, might be the key pathophysiological cause of AD (4).

Focused on the muscle and inflammation alterations in AD, several biomarkers have been found, such as the muscle development-related genes, α-SMA, smMHC, sELAF, PC1 and D-dimer (5); and succinic acid, which participate in p38 MAPK signaling (6).

As one essential protein in maintaining the structural integrity and stability of the vessel wall, PC1, encoded by *PKD1* (Polycystin 1, Transient Receptor Potential Channel Interacting) was verified to regulate the development and progression of TAD via activation of mTOR/S6K/S6 signaling pathway (7). Besides, other research also found that the *PKD1* mediated MEK/ERK/myc signaling pathway (4), which might be the key pathophysiological cause of AD. As a result, *PKD1* showed a multi-potential influence on AD, from muscle and inflammation pathways. However, the major mechanism and interaction network for how *PKD1* regulates AD processing is still unknown, a comprehensive study is needed from the transcriptome profile.

In this study, we compared the normal and AD samples and focused on the variation of correlated genes with *PKD1*, as well as their interaction network. The aim is to expose the major signaling pathway of *PKD1* in AD development and progression, as well as the candidate regulatory network.

Materials and Methods

Dataset
The AD and normal samples used in this study were downloaded from the gene expression omnibus (GEO; GSE153434).

Differential expressed genes (DEGs) detection
The limma package of R was used to screen out DEGs (8). The candidate gene list was assessed by t-test, and Benjamini and Hochberg's method was used to adjust the *P*-value. All DEGs were screened out by the following criteria: at least a 0.8-fold change between healthy controls and AD patient samples and with adjusted $P < 0.05$.

PKD1 co-expressed genes screen
We used the Spearman test to check the co-expression genes of *PKD1*, with a threshold $|r| > 0.5$ and $p < 0.05$. And

* Corresponding author. Email: easylike@163.com

heatmaps were generated using the "heatmap" package of R.

Enrichment analysis

The DAVID v6.8 (9) was used to do the gene ontology annotations, and all categories were divided into the molecular function (MF), biological process (BP) and cell composition (CC). The functional enrichment of the candidate gene list was analyzed by Kobas (10) based on the KEGG database. For both two kinds of enrichment analysis, all significant categories were required to have an adjusted *P*-value below 0.05 in Benjamini and Hochberg's test.

Gene cluster identification and protein-protein interaction (PPI) network analysis

The candidate gene list was applied in the STRING database to obtain the protein network interaction diagram (11), and visualized by Cytoscape v.3.7.1(12). The gene cluster with the highest scores was imported to draw the protein interaction network, and the network was used to determine the hub genes.

Prediction of pivotal miRNAs and construction of gene-miRNA interaction network analysis

Genes related to the crucial pathway were selected and performed with a multiMiR to predict its targeted miRNAs (13). To verify the accuracy of the results, eight databases including DIANA-microT (14), ElMMo (15), MicroCosm (16), Miranda (17), mirdb (18), PicTar (19), PITA (20), and TargetScan (21), were used to do intersection. The result obtained from the intersection was further processed with Cytoscape v3.7.1, and miRNAs were required to target more than two genes.

miRNAs-circRNA prediction

StarBase v2.0 was used to predict the upstream molecules circRNAs of miRNAs, and the obtained data was processed using Cytoscape v3.7.1. The intersection of predicted results of each miRNA was obtained by using the cross-linked graph to identify relevant circRNAs.

Construction of the circRNA-miRNA-mRNA network

circRNA-miRNA pairs and the miRNA-mRNA pairs were integrated, and the nodes that could not accomplish a circRNA-miRNA-mRNA axis were removed. The filtered results were constructed a preliminary circRNA-miRNA-mRNA network, and visualized by Cytoscape v3.7.1.

Statistical Analysis

All bioinformatics analyses in this study were conducted using R software (v.4.0.2). Student T-test was performed for continuous variables. Then, P values were adjusted on the basis of Benjamini and Hochberg's test. Statistically significance was determined so long as p values < 0.05.

Results

Detection of *PKD1*-related differential expressed genes in AD and normal samples.

We collected the expression profile of 20 samples, containing 10 aortic dissection tissue samples and 10 normal tissue samples. A total of 2908 differential expression genes were found, with 1115 genes up-regulated, and 1793 down-regulated in AD samples (Figure 1A, 1B). Notably,
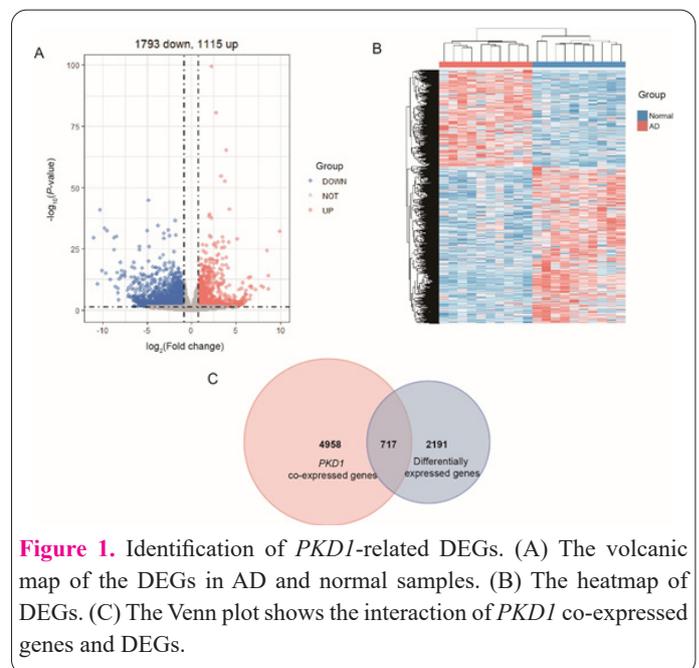

Figure 1. Identification of *PKD1*-related DEGs. (A) The volcanic map of the DEGs in AD and normal samples. (B) The heatmap of DEGs. (C) The Venn plot shows the interaction of *PKD1* co-expressed genes and DEGs.

PKD1 is one down-regulated gene in AD samples with a significant p-value of 0.034 and a $\log_2$ (Fold change) value of -0.82, accordant with previous research (22). To infer the influence of *PKD1* in the development of AD samples, the co-expressed genes with *PKD1* were detected by a Spearman correlation test. 5675 genes showed a high related score with *PKD1*, sharing 717 common genes with DEGs in AD samples (Figure 1C). Among these 717 genes, 85 were up-regulated in AD samples, and 632 were down-regulated.

Transcriptional differences corresponding to *PKD1*-related DEGs

To investigate the potential roles of these 717 genes in AD development, gene ontology enrichment and functional enrichment tests have been done. A total of 50 categories were enriched and kept with a threshold of Corrected *P*-value below 0.05 applied based on Benjamini-Hochberg correction, consisting of 8 in biological process (BP), 32 in cell component and 9 in molecular function (MF) (Figure 2A). In terms of BP, the categories related to muscle development have the highest significant scores, including "skeletal muscle tissue development" (GO:0007519), "negative regulation of smooth muscle cell proliferation" (GO:0048662) and "cellular response to calcium ion" (GO:0071277). Notably, the MF enrichment results also indicated the pivotal changes in VSMCs, all significant MF categories were related to muscle development, as well as calcium ion binding and activity, which play a vital role in VSMCs contraction. Two categories remarkable with the highest gene ratios in CC were also observed, "plasma membrane" (GO:0005886) and "cytoplasm" (GO:0005737). These two enriched components demonstrated that key changes may occur in the membrane and cytoplasm, but not in the nucleus.

The function enrichment showed other key changes in AD development. 717 genes were divided into up-regulated (UP) and down-regulated groups (DOWN), and enriched in the KEGG database, separately. Filtered by the same threshold with GO analysis, 2 categories were retained in the UP group, while 58 were in the DOWN group (Figure 2B). The genes up-regulated focused on the
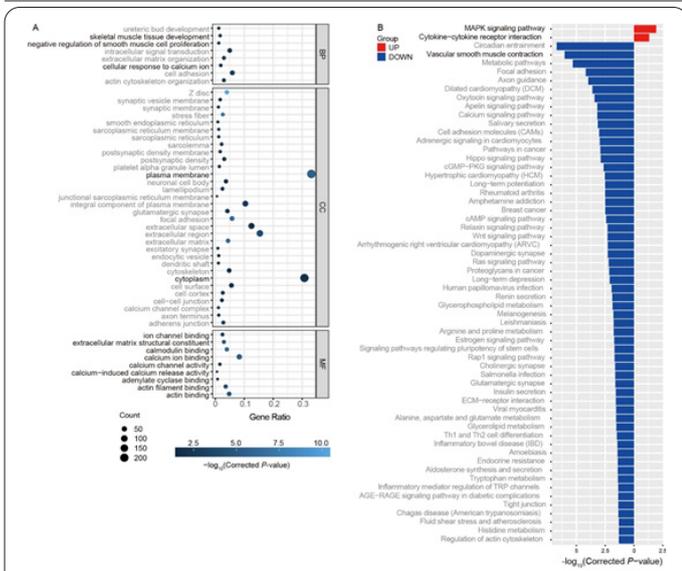
Figure 2. Enrichment analysis for *PKD1*-related DEGs. (A) The GO enrichment results of 717 *PKD1*-related DEGs. The enriched gene numbers are represented by sizes of circles, and -$\log_{10}$ (Corrected *P*-value) by gradation of colors. (B) The bar plot for functional enrichment of 717 *PKD1*-related DEGs. The categories were separated by UP and DOWN groups, shown by red and blue colors. The pathways with black font were mostly discussed.

Figure 3. The interaction network for genes strongly associated with *PKD1*-related DEGs. The gradient of colors represents the correlation score, the darker color means a stronger correlation.

"MAPK signaling pathway" had the highest significant *P*-value, which has been proved in previous research (4). One category in the DOWN group also drew attention, "Vascular smooth muscle contraction", which also has been verified in a previous study (7).

PPI network analysis and detection of hub genes

The 717 genes were utilized to build a protein-protein interaction network referring to the STRING database, containing 500 nodes and 1369 edges. With a threshold of confidence more than 0.9, only two genes *JUN* and *ACTN2* were reserved (Figure 3). *JUN* (Jun Proto-Oncogene), is identified as a major AP-1 family member, and known as an essential regulator of major biological events such as cell proliferation (23). *JUN* is regulated by phosphorylation of its N-terminal activation domain by MAPK (24). *ACTN2* encodes alpha-actinin-2, a protein expressed in human cardiac and skeletal muscle, which may drive the transition of VSMCs to a mechanically stiffer state (25). Both two hub genes participated in the coincident pathways compared with functional enrichment analysis.

Establishment of cicrRNA-miRNA-mRNA interaction network

Using these three genes (*PKD1*, *JUN*, *ACTN2*) as cores, a total of 822 pairs of miRNA-mRNA were detected among 8 databases (Figure 4A). Most pairs were found in Targetscan, with a number of 210. To eliminate the errors, those pairs which only exist in one database were filtered. Among these pairs, 3 miRNAs were remarkable, hsa-miR-625-5P, hsa-miR-1252-5P, and hsa-miR-29b-3p. All of these 3 miRNAs can regulate at least 2 genes through interaction. To figure out the interaction network, circRNA-miRNA pairs were predicted by referring to the Starbase database. 1350, 1918 and 2262 circRNAs for hsa-miR-625-5P, hsa-miR-1252-5P, and hsa-miR-29b-3p were detected respectively. As a result, 7106 circRNA nodes, 3 miRNA nodes, 3 mRNA nodes, and 5537 edges constitu-
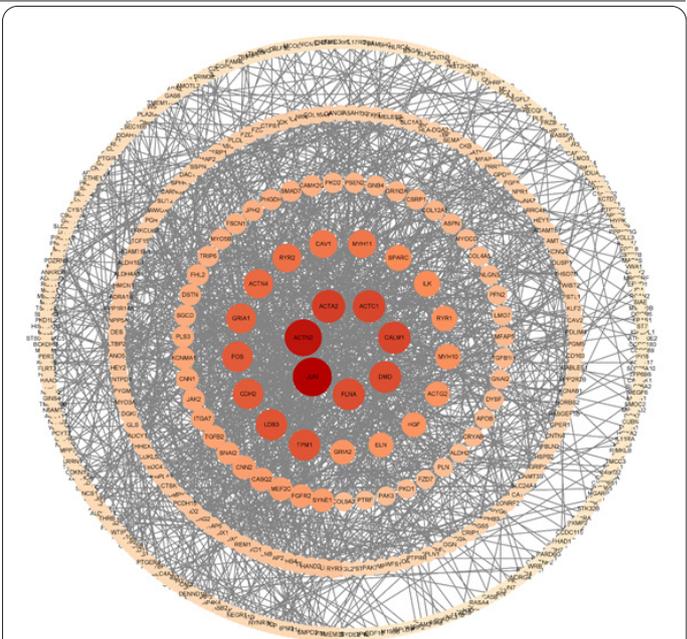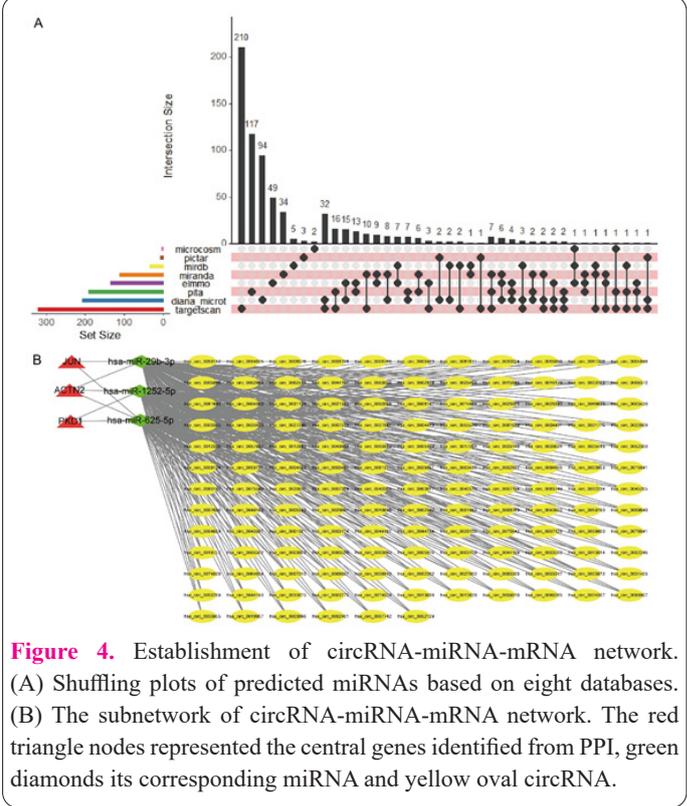

Figure 4. Establishment of circRNA-miRNA-mRNA network. (A) Shuffling plots of predicted miRNAs based on eight databases. (B) The subnetwork of circRNA-miRNA-mRNA network. The red triangle nodes represented the central genes identified from PPI, green diamonds its corresponding miRNA and yellow oval circRNA.

ted the circRNA-miRNA-mRNA network together. A subnetwork that only contained the circRNA of degree 3 was shown (Figure 4B).

Discussion

We have indicated the candidate role of *PKD1* in the pathogenesis of AD, as well as the main pathways, including the decline of VSMCs contraction, the disorder of calcium ion regulation (normal tissue preference), and the enhancement of MAPK signaling (AD tissue preference). Also, we built a *PKD1*-nuclei mRNA-miRNA-circRNA interaction network in AD, demonstrated two hub genes,

and candidate-related miRNAs and circRNAs.

In the previous study, the correlation between PC1 and AD has been observed, for instance, reduced PC1 expression will influence VSMCs phenotypic transition, from contractile to synthetic VSMCs, through mTOR/S6K/S6 signaling pathway (7), and also, PC1 downregulation promoted VSMC proliferation and phenotypic switch, by MEK/ERK/myc pathway (4). Our findings are coordinated with others and give a more comprehensive interpretation of *PKD1* regulation in AD. Moreover, the two hub genes *ACTN2*, and *JUN*, which play important roles in PKD1-AD regulation also supported this result. *ACTN2* plays important structural and functional roles in the sarcomere and contractile apparatus (26). And ACTN1, in the actinin alpha gene family, was proven to interact with *PKD1* (27). While *JUN*, encoding c-JUN protein, is activated by c-Jun N-terminal kinase (JNK)-mediated phosphorylation, which participates in MAPK signaling pathway (28).

It have been widely reported for the coregulation of miRNA and circRNA in AD's development (29). But it is still empty for the *PKD1*-related network in AD. Here, we investigated three candidate key miRNAs, hsa-miR-625-5P, hsa-miR-1252-5P, and hsa-miR-29b-3p. For example, hsa-miR-29b-3p has been verified to target the key genes in vascular smooth muscle contraction as well as the MAPK signaling pathway (30). Additionally, further experiments are still needed to confirm the correlations.

In conclusion, our study provides a more comprehensive understanding for the development and progression of AD, as well as an insight of the role of *PKD1*. The candidate hub genes and cicrRNA-miRNA-mRNA network also complete the genetic basis for further mechanism researches.

Funding

Conflict of Interests

The authors declared no conflict of interest.

References

1. Cottin V, Hirani NA, Hotchkin DL, et al. Presentation, diagnosis and clinical course of the spectrum of progressive-fibrosing interstitial lung diseases. Eur Respir Rev 2018; 27(150):

2. He R, Guo DC, Estrera AL, et al. Characterization of the inflammatory and apoptotic cells in the aortas of patients with ascending thoracic aortic aneurysms and dissections. J Thorac Cardiov Sur 2006; 131(3): 671-678.

3. Jia LX, Zhang WM, Zhang HJ, et al. Mechanical stretch-induced endoplasmic reticulum stress, apoptosis and inflammation contribute to thoracic aortic aneurysm and dissection. J Pathol 2015; 236(3): 373-383.

4. Feng J, Ge S, Zhang L, Che H, Liang C. Aortic dissection is associated with reduced polycystin-1 expression, an abnormality that leads to increased ERK phosphorylation in vascular smooth muscle cells. Eur J Histochem 2016; 60(4): 2711.

5. Peng W, Peng Z, Chai X, et al. Potential biomarkers for early diagnosis of acute aortic dissection. Heart Lung 2015; 44(3): 205-208.

6. Cui H, Chen Y, Li K, et al. Untargeted metabolomics identifies succinate as a biomarker and therapeutic target in aortic aneurysm and dissection. Eur Heart J 2021; 42(42): 4373-4385.

7. Zhang J, Liu F, He YB, et al. Polycystin-1 Downregulation Induced Vascular Smooth Muscle Cells Phenotypic Alteration and Extracellular Matrix Remodeling in Thoracic Aortic Dissection. Front Physiol 2020; 11: 548055.

8. Ritchie ME, Phipson B, Wu D, et al. limma powers differential expression analyses for RNA-sequencing and microarray studies. Nucleic Acids Res 2015; 43(7): e47.

9. Sherman BT, Hao M, Qiu J, et al. DAVID: a web server for functional enrichment analysis and functional annotation of gene lists (2021 update). Nucleic Acids Res 2022; 50(W1): W216-W221.

10. Bu D, Luo H, Huo P, et al. KOBAS-i: intelligent prioritization and exploratory visualization of biological functions for gene enrichment analysis. Nucleic Acids Res 2021; 49(W1): W317-W325.

11. Szklarczyk D, Morris JH, Cook H, et al. The STRING database in 2017: quality-controlled protein-protein association networks, made broadly accessible. Nucleic Acids Res 2017; 45(D1): D362-D368.

12. Shannon P, Markiel A, Ozier O, et al. Cytoscape: a software environment for integrated models of biomolecular interaction networks. Genome Res 2003; 13(11): 2498-2504.

13. Ru Y, Kechris KJ, Tabakoff B, et al. The multiMiR R package and database: integration of microRNA-target interactions along with their disease and drug associations. Nucleic Acids Res 2014; 42(17): e133.

14. Paraskevopoulou MD, Georgakilas G, Kostoulas N, et al. DIANA-microT web server v5.0: service integration into miRNA functional analysis workflows. Nucleic Acids Res 2013; 41(Web Server issue): W169-W173.

15. Gaidatzis D, van Nimwegen E, Hausser J, Zavolan M. Inference of miRNA targets using evolutionary conservation and pathway analysis. Bmc Bioinformatics 2007; 8(69).

16. Griffiths-Jones S, Saini HK, van Dongen S, Enright AJ. miRBase: tools for microRNA genomics. Nucleic Acids Res 2008; 36(Database issue): D154-D158.

17. Enright AJ, John B, Gaul U, Tuschl T, Sander C, Marks DS. MicroRNA targets in Drosophila. Genome Biol 2003; 5(1): R1.

18. Chen Y, Wang X. miRDB: an online database for prediction of functional microRNA targets. Nucleic Acids Res 2020; 48(D1): D127-D131.

19. Krek A, Grun D, Poy MN, et al. Combinatorial microRNA target predictions. Nat Genet 2005; 37(5): 495-500.

20. Kertesz M, Iovino N, Unnerstall U, Gaul U, Segal E. The role of site accessibility in microRNA target recognition. Nat Genet 2007; 39(10): 1278-1284.

21. Agarwal V, Bell GW, Nam JW, Bartel DP. Predicting effective microRNA target sites in mammalian mRNAs. Elife 2015; 4:

22. Zhang L, Yu C, Chang Q, Luo X, Qiu J, Liu S. Comparison of gene expression profiles in aortic dissection and normal human aortic tissues. Biomed Rep 2016; 5(4): 421-427.

23. Shaulian E, Karin M. AP-1 in cell proliferation and survival. Oncogene 2001; 20(19): 2390-2400.

24. Pulverer BJ, Kyriakis JM, Avruch J, Nikolakaki E, Woodgett JR. Phosphorylation of c-jun mediated by MAP kinases. Nature 1991; 353(6345): 670-674.

25. Qian W, Hadi T, Silvestro M, et al. Microskeletal stiffness promotes aortic aneurysm by sustaining pathological vascular smooth muscle cell mechanosensation via Piezo1. Nat Commun 2022; 13(1): 512.

26. Harper SQ, Crawford RW, DelloRusso C, Chamberlain JS. Spectrin-like repeats from dystrophin and alpha-actinin-2 are not functionally interchangeable. Hum Mol Genet 2002; 11(16): 1807-1815.

27. Geng L, Burrow CR, Li HP, Wilson PD. Modification of the com-

position of polycystin-1 multiprotein complexes by calcium and tyrosine phosphorylation. Biochim Biophys Acta 2000; 1535(1): 21-35.

28. Davies C, Tournier C. Exploring the function of the JNK (c-Jun N-terminal kinase) signalling pathway in physiological and pathological processes to design novel therapeutic strategies. Biochem Soc T 2012; 40(1): 85-89.

29. Shen L, Hu Y, Lou J, et al. CircRNA-0044073 is upregulated in atherosclerosis and increases the proliferation and invasion of cells by targeting miR-107. Mol Med Rep 2019; 19(5): 3923-3932.

30. Marttila S, Rovio S, Mishra PP, et al. Adulthood blood levels of hsa-miR-29b-3p associate with preterm birth and adult metabolic and cognitive health. Sci Rep-Uk 2021; 11(1): 9203.